DALTON
FULL PAPER

Towards nanostructured arrays of single molecule magnets: new Fe_{19} oxyhydroxide clusters displaying high ground state spins and hysteresis †

Jeremy C. Goodwin,[a] Roberta Sessoli,[c] Dante Gatteschi,[c] Wolfgang Wernsdorfer,[d] Annie K. Powell *[b] and Sarah L. Heath *[a]

[a] *Department of Chemistry, University of York, Heslington, York, UK YO10 5DD. E-mail: slh11@york.ac.uk*
[b] *Institut für Anorganische Chemie, Universität Karlsruhe, Engesserstr. Geb. 30.45, D-76128 Karlsruhe, Germany*
[c] *Dipartimento di Chimica, Universita degli Studi di Firenze, Via Maragliano 77, 50144 Firenze, Italy*
[d] *Laboratoire Louis Neél, CNRS, 25 Avenue des Martyrs BP166, 38042 Grenoble Cedex 9, France*

Received 16th March 2000, Accepted 28th April 2000
Published on the Web 26th May 2000

Ligands of general formula $N(CHRCH_2OH)(CH_2CO_2H)_2$ have been used to capture portions of the $Fe(OH)_2^+$ lattice to give particles containing up to nineteen magnetically coupled iron(III) centres. If R = Me or Et, lattices containing only Fe_{19} clusters result and single crystal X-ray diffraction shows that these are arranged in tilted stacks. These clusters act as single molecule magnets, pointing the way forward to engineering ordered arrays of magnetic particles. The packing of such materials is independent of the counter anion, NO_3^- or Cl^-, used.

Introduction

The current interest in synthesizing molecular-based magnets stems in part from the desire to design new materials for data storage applications. Many of these are based on engineered infinite arrays of interacting paramagnets,[1] whilst a smaller number comprise discrete aggregates of transition metal ions.[2] Following on from our work on the Fe_{17}/Fe_{19} system with the ligand H_3heidi,[3,4] we have been exploring ways of creating engineered infinite arrays of such zero-dimensional (nanoscale) aggregates. We demonstrated that the ligand was capable of capturing iron hydroxide frameworks related to "laboratory rust", $Fe(OH)_3$, which is the usual product of hydrolysis of Fe(III) (hence our colloquial name of "crusts" for these materials) and in the Fe_{17}/Fe_{19} case we found that there were two interpenetrating lattices of Fe_{17} and Fe_{19} clusters (Fig. 1a). Although within each lattice the clusters are arranged in parallel stacks, these are oriented at 28° to each other and this, in conjunction with a complicated hydrogen-bonding network, makes the interpretation of the magnetic data very difficult.[4] Nevertheless, the magnetic measurements we have performed indicate that such systems stabilise high ground state spins and display hysteresis phenomena at low temperatures.[5] Although this behaviour is only manifest at temperatures too low to be useful for direct applications, it is a clear indication of the potential of such systems in areas such as quantum devices, where zero-dimensional systems are required. A further problem with the Fe_{17}/Fe_{19} system is that it is not soluble in any common solvent and when interacted with water it evolves into the dimer $[Fe(heidi)(H_2O)]_2$ and some form of iron oxyhydroxide material. In order to explore the way in which crystal packing and cluster solubility can be modulated, we have been modifying the alcohol side arm of the parent ligand H_3heidi and report here the results we have obtained for metheidi and etheidi. We have also monitored the effect the counter anion might have on the crystal structure by comparing materials with nitrate and chloride counter ions. Our aim in doing this has been to find ways to modify the supramolecular interactions in the lattices with the idea of creating oriented arrays of magnetic particles. As a starting point it seemed logical to explore how small modifications to the parent H_3heidi ligand, which we know can stabilise relatively large iron(III) oxyhydroxide aggregates, might modulate such supramolecular effects. Our ultimate goal in this is to produce structured arrays of nanoparticles displaying the unusual properties associated with zero-dimensional systems. In this case we have chosen to monitor the anomalous magnetic behaviour such particles can display, and which we have already observed in the Fe_{19}/Fe_{17} system, in order to gauge the utility of our approach.

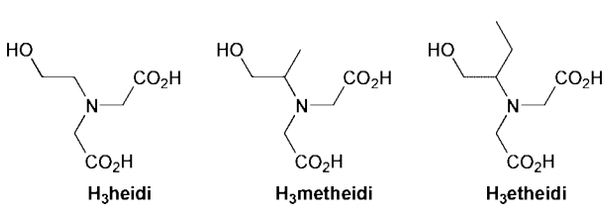

Experimental

All reagents were used as received from Aldrich Chemicals. ^{1}H NMR spectra were recorded on a Bruker DPX250 spectrometer. Magnetisation measurements were performed on a Metronique MS02 magnetometer on polycrystalline powder embedded in epoxy glue to avoid orientation. Measurements below 1 K were performed on a single crystal using a home made μ-SQUID's magnetometer.[6] High Field EPR spectra were recorded on a laboratory-made spectrometer[7] where the radiation sources are Gunn diodes equipped with frequency multipliers and the absorption of the far-infrared radiation is detected with a bolometer.

† This paper is dedicated to the late Olivier Kahn.

DOI: 10.1039/b002135k

Preparations

***N*-(1-Hydroxymethylethyl)iminodiacetic acid (H_3metheidi).** DL-2-Amino-1-propanol (7.50 g, 0.1 mol), ethyl bromoacetate (33.4 g, 0.2 mol) and potassium hydrogencarbonate (20.02 g, 0.2 mol) were refluxed in EtOH (100 mL) for 24 hours. The solid KBr was filtered off and the solvent removed *in vacuo*. The resultant yellow oil was refluxed in water (80 mL) and 5 mL 37% HCl for 24 hours. The solution was then reduced to 25 mL. A white crystalline solid formed after one week (7.43 g, 39%) (Found: C, 43.20; H, 6.94; N, 7.19. $C_7H_{13}NO_5$ requires C, 43.98; H, 6.81; N, 7.33%). ^{1}H NMR (270 MHz, solvent D_2O): δ 1.25 (3 H, d, CH_3), 3.70 (1 H, m, CH), 3.85 (2 H, d, CH_2) and 4.00 (4 H, s, CH_2).

***N*-(1-Hydroxymethylpropyl)iminodiacetic acid (H_3etheidi).** This was prepared using the same method as for H_3metheidi, using DL-2-amino-1-butanol (8.91 g, 0.1 mol). After two days a white crystalline solid formed (10.12 g, 49%) (Found: C, 46.83; H, 7.48; N, 6.77. $C_8H_{15}NO_5$ requires C, 46.83; H, 7.32; N, 6.83%). ^{1}H NMR (270 MHz, solvent D_2O): δ 1.00 (3 H, t, CH_3), 1.70 (2 H, m, CH_2), 3.45 (1 H, m, CH), 3.70 (2 H, m, CH_2) and 4.00 (4 H, s, CH_2).

$[Fe_{19}(metheidi)_{10}(OH)_{14}(O)_6(H_2O)_{12}]NO_3\cdot 24H_2O$ 1. To a solution of $Fe(NO_3)_3\cdot 9H_2O$ (2.01 g, 5 mmol) in water (10 mL) a solution of H_3metheidi (0.48 g, 2.5 mmol) and pyridine (1.21 mL, 15 mmol) in water (10 mL) was added with stirring. The resultant red solution, pH 3.41, was left to crystallise, forming brown needles suitable for single crystal X-ray diffraction in 24 hours (0.45 g, 34%) (Found: C, 21.55; H, 4.51; Fe, 26.00; N, 4.35. $C_{70}H_{186}Fe_{19}N_{11}O_{109}$ requires C, 21.09; H, 4.70; Fe, 26.61; N, 3.86%).

$[Fe_{19}(etheidi)_{10}(OH)_{14}(O)_6(H_2O)_{12}]NO_3\cdot 18H_2O$ 2. To a solution of $Fe(NO_3)_3\cdot 9H_2O$ (2.01 g, 5 mmol) in water (10 mL) a solution of H_3etheidi (0.48 g, 2.5 mmol) and pyridine (1.21 mL, 15 mmol) in water (10 mL) was added with stirring. The resultant red solution, pH 3.19, was left to crystallise, forming tiny brown needles suitable for single crystal X-ray diffraction in 4 hours (0.35 g, 43%) (Found: C, 23.30; H, 5.02; Fe, 25.57; N, 3.68. $C_{80}H_{194}Fe_{19}N_{11}O_{103}$ requires C, 23.91; H, 4.87; Fe, 25.40; N, 3.83%).

$[Fe(metheidi)(H_2O)]_2\cdot 4H_2O$ 3. To a solution of $Fe(NO_3)_3\cdot 9H_2O$ (1.01 g, 2.5 mmol) in water (10 mL) a solution of H_3metheidi (0.48 g, 2.5 mmol) and NaOH (0.2 g, 5 mmol) in water (10 mL) was added with stirring. The resultant yellow solution, pH 1.52, was left to crystallise by slow evaporation, forming green blocks suitable for single crystal X-ray diffraction (0.22 g, 29%) (Found: C, 28.83; H, 5.45; Fe, 18.85; N, 4.67. $C_7H_{16}FeNO_8$ requires C, 28.19; H, 5.41; Fe; 18.77; N, 4.70%).

$[Fe(etheidi)(H_2O)]_2$ 4. To a solution of $Fe(NO_3)_3\cdot 9H_2O$ (1.01 g, 2.5 mmol) in water (10 mL) a solution of H_3etheidi (0.48 g, 2.5 mmol) and NaOH (0.2 g, 5 mmol) in water (10 mL) was added with stirring. The resultant yellow solution, pH 1.70, was left to crystallise, forming green spheroids in five weeks, not suitable for X-ray analysis (0.49 g, 71%) (Found: C, 34.50; H, 4.87; Fe, 19.95; N, 5.08. $C_8H_{14}FeNO_6$ requires C, 34.80; H, 5.11; Fe, 20.23; N, 5.07%).

$[Fe_{19}(metheidi)_{10}(OH)_{14}(O)_6(H_2O)_{12}]Cl\cdot 31.5H_2O$ 5. To a solution of hydrated $FeCl_3\cdot 6H_2O$ (1.35 g, 5 mmol) in water (10 mL) a solution of H_3metheidi (0.48 g, 2.5 mmol) and pyridine (1.21 mL, 15 mmol) in water (10 mL) was added with stirring. The resultant red solution, pH 3.51, was left to crystallise, forming brown needles suitable for single crystal X-ray diffraction in 24 hours (0.29 g, 27%) (Found: C, 20.88; H, 4.80; N, 3.27. $C_{70}H_{201}ClFe_{19}N_{10}O_{113.5}$ requires C, 20.53; H, 4.95; N, 3.42%).

$[Fe_{19}(etheidi)_{10}(OH)_{14}(O)_6(H_2O)_{12}]Cl\cdot 48.5H_2O$ 6. To a solution of hydrated $FeCl_3\cdot 6H_2O$ (1.35 g, 5 mmol) in water (10 mL) a solution of H_3etheidi (0.51 g, 2.5 mmol) and pyridine (1.21 mL, 15 mmol) in water (10 mL) was added with stirring. The resultant red solution, pH 3.53, was left to crystallise, forming tiny brown needles suitable for single crystal X-ray diffraction in 4 hours (0.24 g, 20%) (Found: C, 21.55; H, 5.34; N, 3.31. $C_{80}H_{255}ClFe_{19}N_{10}O_{130.5}$ requires C, 21.15; H, 5.66; N, 3.08%).

X-Ray crystallography

Single crystals suitable for X-ray diffraction studies were obtained for compounds **1**–**3**, **5** and **6**; those of **2** were extremely small (0.21 × 0.06 × 0.04 mm) and weakly diffracting and the data were not of sufficient quality to allow complete X-ray analysis of the structure. Data were collected at 150 K on a Bruker SMART 1000 CCD diffractometer equipped with an Oxford Cryostreams low temperature attachment. The structures were solved by direct methods and refined on F^2 using SHELXL 97 software.[8] To preserve a reasonable data : parameter ratio only the iron atoms of **2** were refined anisotropically. However, the unit cell of the structure was determined to a high accuracy and the data are sufficient to allow for the location of the Fe_{19} clusters and perform the analysis of the gross packing of the structure. The structural analyses on compounds **5** and **6** were carried out to gauge the effect the counter anion might have on the crystal packing. For compounds **1**, **2**, **5** and **6** the presence of both enantiomers is evidenced by disorder in the alcohol arm of the ligand. Crystal data are summarised in Table 1.

CCDC reference number 186/1957.

See http://www.rsc.org/suppdata/dt/b0/b002135k/ for crystallographic files in .cif format.

Results and discussion

X-Ray crystallographic analyses of the products of the reactions of one equivalent of H_3metheidi, **1**, or H_3etheidi, **2**, with two equivalents of iron(III) nitrate nonahydrate reveal the formation of lattices containing exclusively Fe_{19} clusters (Fig. 2), isostructural with the Fe_{19} heidi cluster reported by us previously.[3] As before, the clusters carry a charge of +1 which is balanced by a nitrate counter ion. Thus, the unit cells of **1** and **2** contain one cluster and one nitrate anion with twenty four waters of crystallisation for the metheidi cluster and eighteen for the etheidi cluster. This is in contrast to the original iron/heidi clusters where the unit cell contained one Fe_{19} and one Fe_{17} cluster, four nitrate anions and approximately sixty waters of crystallisation. This leads to smaller unit cell volumes for **1** and **2** compared with the Fe/heidi system as a consequence of having one lattice of parallel columns of Fe_{19} clusters (Fig. 1b) rather than two interpenetrating lattices of Fe_{19} and Fe_{17} clusters (Fig. 1a).

For compounds **1** and **2** the iron atoms at the centre of the disks are at the unit cell corners. The disks lie in planes defined approximately by the {110} plane for **1** and $\{1\bar{1}0\}$ plane for **2**. Within these planes, for compound **1**, the centres of these disks are 17.60 (the *c* axis) and 20.15 Å (the shortest diagonal of the *ab* face) apart, subtending an angle of 79.4°, with the planes spaced at 11.28 Å (Fig. 3 and Table 2). For compound **2** the centres of the disks are 18.62 (the *c* axis) and 20.39 Å (the shortest diagonal of the *ab* face) apart, subtending an angle of 69.1° with the planes spaced at 11.16 Å. The increased distances of the *c* axis, and the *ab* diagonal for compound **2**, are a consequence of the longer aliphatic chain, with the *c* axis representing the closest cluster–cluster approach possible to accommodate the aliphatic side chains of the modified heidi ligands. Compounds **5** and **6** also show the same gross packing indicating that it is the clusters rather than the counter ions which are

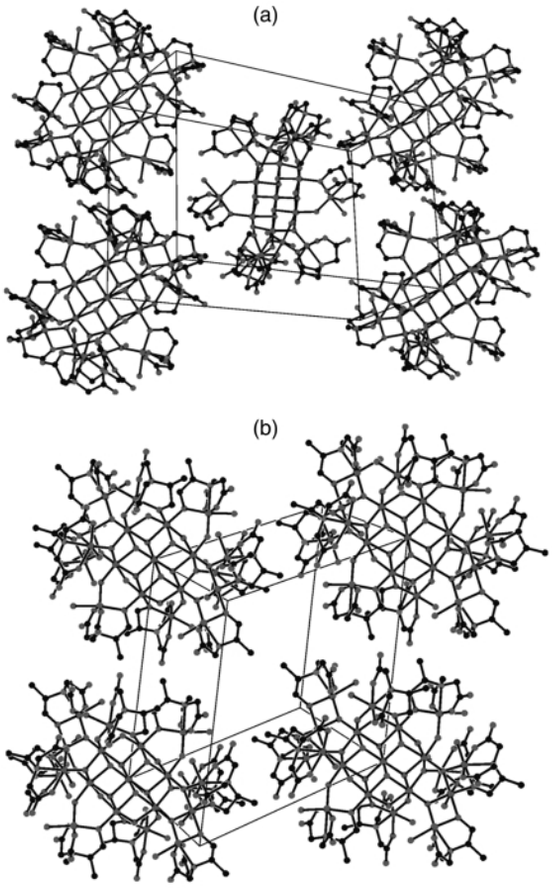

Fig. 1 Packing diagrams of (a) the Fe_{17}/Fe_{19} heidi system and (b) compound **1**.

the major factor in dictating the packing arrangement with the disks lying approximately in the $\{\bar{1}\bar{1}0\}$ and $\{1\bar{1}0\}$ planes respectively. The metrical details are summarised in Table 2.

From Table 2 we can see the beginnings of a trend towards hexagonal packing of the disks emerging as the chain length on the ligand backbone increases. Ideally, we would expect the acute angle to be 60° and the obtuse 120° in regular hexagonal packing within the planes of the disks. For both metheidi compounds, **1** and **5**, the angle is more acute than for the corresponding etheidi compound, although it is interesting that both the chloride derived systems, **5** and **6**, display parameters closer to those for hexagonal packing than the nitrate counterparts. Ideally, a large sample set of analogues with increasing chain lengths and a variety of counter anions would be produced and crystallographically characterised in order to judge whether these trends persist. However, intuition would suggest that increasing chain length, and therefore steric interactions, should make space for the disks to pack hexagonally, and we can also expect that, whilst the effects might be much more subtle, counter anions can have an influence on the detailed packing through hydrogen bonding interactions mediated by lattice waters and peripheral carbonyl groups on the ligands. This indicates means for engineering a lattice with widely spaced clusters, thereby reducing and eventually eliminating, cluster–cluster interactions. An additional benefit of adding longer aliphatic chains to the periphery of the clusters is the likelihood of improving their solubility. These factors could be important in certain aspects of nanotechnology where discrete monodispersed particles are required.

The modification of the substituent group on the three ligands also affects the way in which the clusters form. In the case of the heidi clusters, product is precipitated after twenty minutes and subsequently the alkoxo-bridged dimer $[Fe(heidi)(H_2O)]_2$ is formed. Any slight perturbations in the reaction conditions lead exclusively to the formation of the dimer.[3,4] However, in the case of metheidi and etheidi, the clusters crystallise after 24 and 4 hours respectively and the reaction conditions can be subject to quite large perturbations. This trend is observed with both the counter ions, indicating that it is the ligand, and not the counter ion, which is controlling the rate of formation of the clusters. The reasons for this are not entirely clear, but it is apparent that relatively small changes to the ligand backbone can influence properties such as solubility and crystal packing. The crystal structure of the alkoxo-bridged dimer $[Fe(metheidi)(H_2O)]_2$ **3** reveals it to be isostructural with the Fe/heidi dimer. The dimer unit of **3** is produced by inverting the asymmetric unit, $\{Fe(metheidi)(H_2O)\}$, about a crystallographic inversion centre positioned on the centroid of Fe(1), O(1), Fe(1A), O(1A), Fig. 4. This generates two chemically and

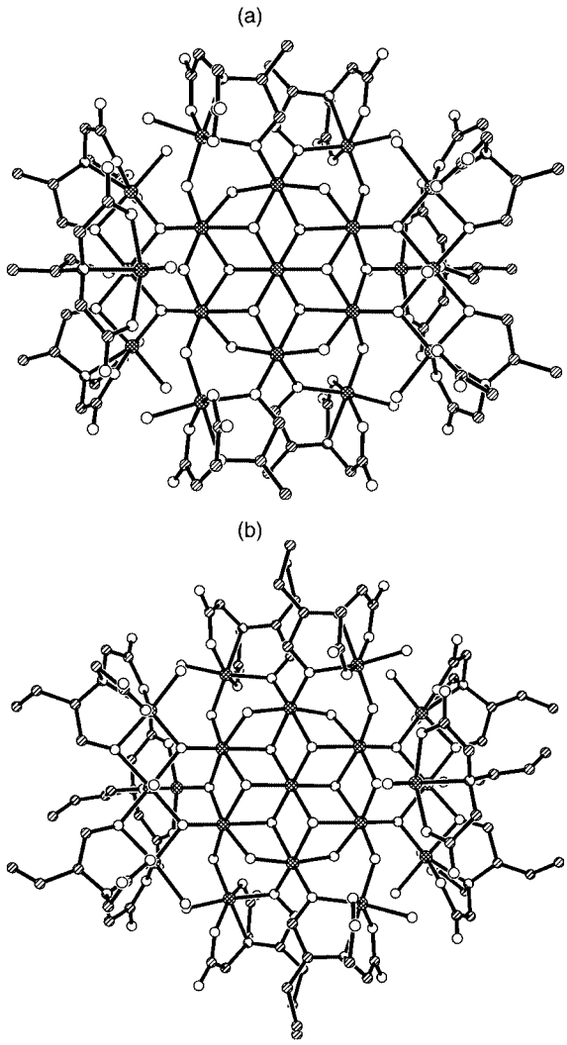

Fig. 2 Crystal structures of (a) $[Fe_{19}(metheidi)_{10}(\mu_3\text{-}OH)_6(\mu\text{-}OH)_8(\mu_3\text{-}O)_6(H_2O)_{12}]^+$ **1** and (b) $[Fe_{19}(etheidi)_{10}(\mu_3\text{-}OH)_6(\mu\text{-}OH)_8(\mu_3\text{-}O)_6(H_2O)_{12}]^+$ **2**. Key: Fe (cross-hatched circles), O (open circles), carbon (shaded top right to bottom left) and nitrogen (shaded circle with highlight).

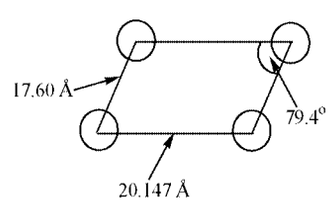

Fig. 3 View of the 110 plane for compound **1** showing the Fe_{19} clusters as stylised disks.

Table 1 Crystal data for compounds **1**–**3**, **5** and **6**

	1	**2**	**3**	**5**	**6**
Chemical formula	$C_{70}H_{186}Fe_{19}N_{11}O_{109}$	$C_{80}H_{194}Fe_{19}N_{11}O_{103}$	$C_{14}H_{32}Fe_2N_2O_{16}$	$C_{70}H_{201}ClFe_{19}N_{10}O_{113.5}$	$C_{80}H_{255}ClFe_{19}N_{10}O_{130.5}$
Formula weight	3987.45	4019.61	596.12	4096.01	4542.54
Crystal system	Triclinic	Triclinic	Triclinic	Triclinic	Triclinic
Space group	$P\bar{1}$	$P\bar{1}$	$P\bar{1}$	$P\bar{1}$	$P\bar{1}$
a/Å	13.309(3)	13.044(3)	6.9549(8)	13.3960(8)	13.4249(14)
b/Å	17.273(5)	17.624(4)	9.3819(11)	17.6134(11)	18.7748(19)
c/Å	17.600(4)	18.621(4)	9.9130(12)	19.0634(11)	20.099(2)
α/°	65.201(10)	110.472(4)	67.995(2)	108.7310(10)	117.717(2)
β/°	74.514(6)	94.820(5)	88.680(2)	95.0490(10)	91.271(2)
γ/°	81.300(2)	98.137(4)	74.027(2)	97.9560(10)	91.711(2)
V/Å^3	3535.8(14)	3928.5(16)	574.22(12)	4176.5(4)	4479.0(8)
Z	1	1	1	1	1
μ/mm^{-1}	2.008	1.805	1.344	1.629	1.619
Reflections collected	23499	49820	3180	27770	29833
(R_{int})	0.0526	0.3166	0.0646	(0.0743)	0.0463
Independent reflections	16132	18893	2620	19085	20546
Final $R1$, $wR2$	0.0536, 0.1235	0.1097, 0.2493	0.0488, 0.1192	0.0734, 0.2143	0.0668, 0.1577
(Reflections [$I > 2\sigma(I)$])	(8837)	(3737)	(2149)	(11334)	(9640)
Parameters	1044	496	172	1078	1034
Final $R1$, $wR2$ (all data)	0.1100, 0.1418	0.4014, 0.3579	0.0608, 0.1242	0.1185, 0.2463	0.1502, 0.1860

Table 2 Intra-cluster geometries for compounds **1**, **2**, **5** and **6**

	1	**2**	**5**	**6**
Shortest interdisk approach (c axis)[a]/Å	17.60	18.62	19.06	20.10
Longest interdisk approach (ab diagonal)[a]/Å	20.15	20.39	20.60	23.41
Acute subtending angle[a]/Å	79.4	69.1	70.6	68.9
Obtuse subtending angle/°	100.6	110.9	109.4	111.1
Distance between planes[a]/Å	11.28	11.16	11.35	10.77

[a] As defined in Fig. 3.

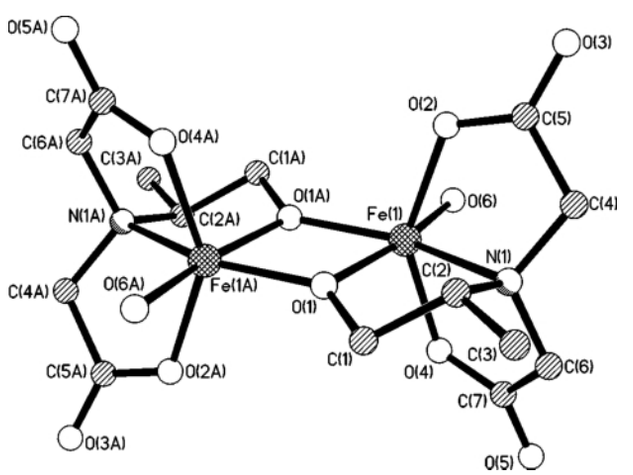

Fig. 4 Crystal structure of $[Fe(metheidi)(H_2O)]_2$ **3**.

crystallographically equivalent iron(III) ions which are bridged by the deprotonated alkoxyl group of the ligand, O(1) and O(1A). IR and microanalytical data indicate that it is also possible to synthesize an etheidi alkoxo-bridged dimer, $[Fe(etheidi)(H_2O)]_2$ **4**. Both these dimers can be isolated using the conventional dimer synthesis as reported for the Fe/heidi dimer from all iron(III) starting materials.[3,4]

Magnetic studies were performed on compounds **1** and **2** as "parents" of this series. The product $\chi_m T$ increases on lowering the temperature for both as has been observed in the Fe_{19}/Fe_{17} system. The highest temperature value is *ca.* 43 emu K mol^{-1} for both compounds, a value significantly smaller than that expected for 19 uncorrelated $S = 5/2$ spins with $g = 2$, $\chi_m T = 83.125$ emu K mol^{-1}, suggesting the presence of a range of antiferromagnetic pairwise interactions that give rise to an

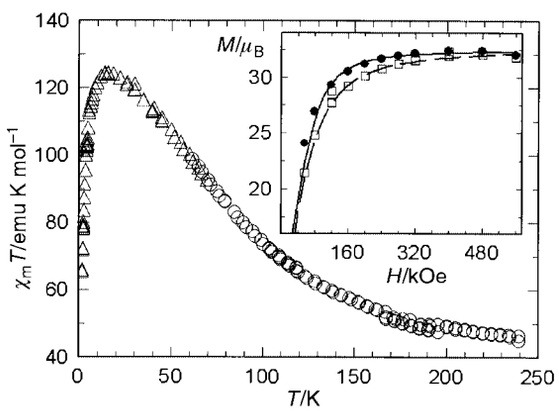

Fig. 5 Temperature dependence of the product of the magnetic susceptibility with temperature reported per mol of cluster **1**, measured at 10 kOe down to 60 K (circles) and 500 Oe below 60 K (triangles). The inset shows the magnetisation measured at 2.45 (●) and 4.4 K (□). The lines have been calculated using $S = 33/2$, $D = -0.04$ cm^{-1}, and $g = 1.96$.

uncompensated magnetic moment. Both compounds show a maximum in $\chi_m T$ at *ca.* 15 K with corresponding $\chi_m T$ values of 127 and 124 emu K mol^{-1} for **1** and **2** respectively. A rapid decrease is observed on lowering the temperature further, as shown in Fig. 5 for **1**. Such a decrease could be due to the presence of magnetic anisotropy (zero-field splitting of the ground S state) and/or to weak intercluster interactions.

The temperature dependence of the susceptibility below 15 K can reasonably be approximated to a Curie–Weiss behaviour with $C = (Ng^2\mu_B{}^2/3k_B)S(S + 1) = 143(3)$ emu K mol^{-1} for compound **1**, which is not far from the value expected for $S = 33/2$ (144.4 emu K mol^{-1} for $g = 2$), and a negative Weiss temperature $\theta = -1.7$ K, indicative of weak antiferromagnetic inter-cluster interactions. The value of S was not too far from that predicted ($S = 35/2$) for the Fe_{19} moiety in the Fe_{19}/Fe_{17} compound.[4,5] For **2** C was found to be 137 emu K mol^{-1}, which lies between $S = 31/2$ and 33/2, and weaker intermolecular antiferromagnetic interactions, $\theta = -1.4$ K, are observed. These values are consistent with the fact that there are larger intercluster separations in **2**. The presence of magnetic anisotropy can however also affect the C and θ values.

The field dependence of the magnetisation measured for compound **1** at 2.45 and 4.40 K is shown in the inset of Fig. 5. The magnetisation is saturated at the highest field of 70 kOe with a value of *ca.* 32.5 μ_B for **1**, in good agreement with the expected value for $S = 33/2$ with $g = 2$. The curves can reason-

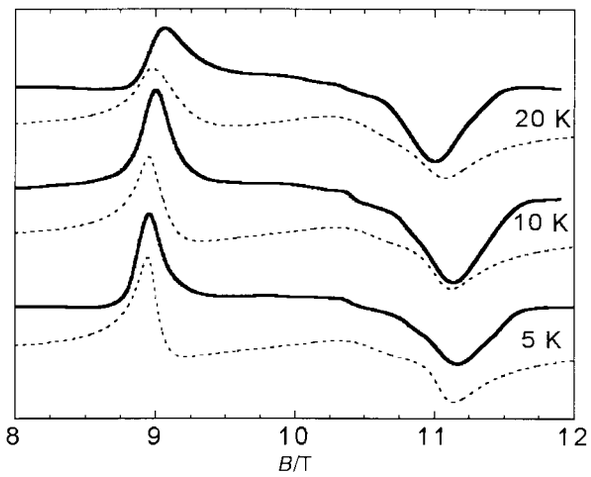

Fig. 6 High field EPR spectra recorded at three temperatures and 285 GHz on a polycrystalline powder of compound **1** pressed in a pellet. The dotted lines are the simulated spectra assuming an isotropic $g = 2$, $S = 33/2$, $D = -0.035$ cm^{-1}, $E = 0.005$ cm^{-1}, $\Delta B_x = 150$ mT, $\Delta B_y = 300$ mT, and $\Delta B_z = 60$ mT. The $g = 2$ resonates at 10.18 T.

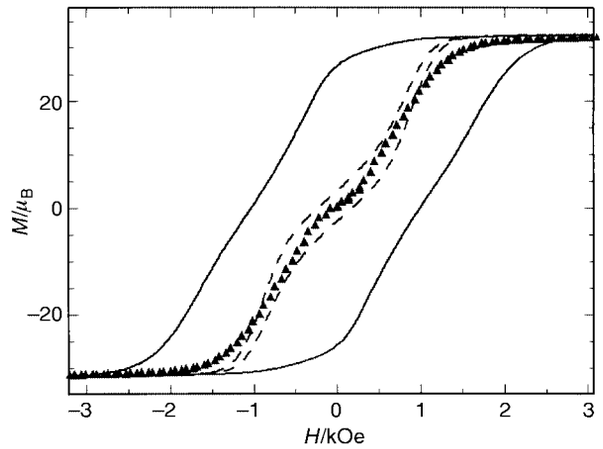

Fig. 7 Magnetic hysteresis cycles measured on a single crystal of compound **1** at 1.1 (triangles), 0.5 (broken line), and 0.3 K (solid line).

ably be simulated by introducing a small axial zero-field splitting, as shown in the inset of Fig. 5, where the parameters $S = 33/2$ and $D = -0.04$ cm^{-1}, and $g = 1.96$ are used. However, the D parameter is only approximate due to the presence of inter-cluster interactions. For compound **2** a saturation value of 31 μ_B is observed in better agreement with $S = 31/2$, but the Curie constant is significantly larger than the calculated one for this spin value leaving an ambiguity on the assignment of the spin of the ground state.

In order to try to quantify the zero-field splitting parameters, high-frequency EPR spectra were recorded on polycrystalline powder samples of compounds **1** and **2** pressed into a pellet. For the two Fe_{19} derivatives examined the spectra obtained at 285 GHz and low temperatures (between 5 and 20 K) present very similar shapes and the spectra for **1** are shown in Fig. 6. Essentially, these spectra look like powder spectra of a spin equals $\frac{1}{2}$ with almost axial anisotropy, showing a parallel signal at low field (8.95 T for **1** and 9.09 T for **2** at 5 K) and a high field signal close to 10.9 T for **1** and 10.7 T for **2**. This anisotropy of the spectra is a result of the crystal field splitting of the large spin ground state and the large magnetic field employed.[9] Indeed at 5 K in a strong magnetic field only the lowest M levels of the spin multiplet are thermally populated and the signal observed corresponds essentially to the transition from the $M = -S$ to $M = -S + 1$ for each principal axis. As the temperature is increased more levels are populated and more transitions contribute to the spectrum. However, in these samples, the small separation between the lines is comparable to the linewidth and we do not observe a clear multiplet pattern but only a shift of the signals towards the centre of the spectrum ($g = 2$ at 10.18 T for 285 GHz). The parallel signal is found at low field, in agreement with a negative D value.

In order to obtain a better estimation of the parameters describing the ground spin state, we simulated the spectra using a program that diagonalises the matrices describing the Hamiltonian of the system, eqn. (1), where g is the Landé

$$H = g\mu_B \mathbf{S}\cdot\boldsymbol{B}_0 + D[S_z^2 - \tfrac{1}{3}S(S+1)] + E(S_x^2 - S_y^2) \quad (1)$$

factor, μ_B the Bohr magneton, S_i the spin operator, $\boldsymbol{B}_0$ the external magnetic field, and D and E are the axial and rhombic contributions of the zero-field splitting. Owing to the very large spin value we had to restrict the simulations to only the allowed transitions, which is reasonable in this case as the D value is small compared to the Zeeman interaction. For compound **1** the spectra were simulated with the parameters $S = 33/2$, $g = 2.0$ (reasonable for high spin iron(III)), $D = -0.035$ cm^{-1} and $E = 0.005$ cm^{-1}, which are in good agreement with the set of parameters used to reproduce the magnetisation curves at low temperature. The experimental spectra show a larger shift towards the centre of the spectrum on increasing the temperature which is probably due to the population of the excited spin levels with smaller S. Other spin ground states like $S = 31/2$ or 35/2 with slightly different zero-field splitting parameters can give similar simulated spectra. As the single $M \longrightarrow M + 1$ transitions are not resolved they cannot be enumerated in order to assign an unambiguous value of S for compound **2**.

For negative D values the $M = \pm 33/2$ states lie lowest in energy and to reverse the magnetisation a barrier must be overcome, whose height is given by the difference between $M = \pm 33/2$ and $\pm 1/2$, $\Delta E = |D|((33/2)^2 - 1/4)$.[9] For **1** we evaluate an energy barrier of 15.7 K and therefore slow relaxation of the magnetisation could occur at low temperature as observed for other high spin molecular clusters.[5,7,10] Compound **1** indeed behaves as a single molecule magnet as shown by the presence of magnetic hysteresis below 1 K detected by using a μ-SQUID's magnetometer. The curves, shown in Fig. 7, reveal a decrease of the slope around $H = 0$ which could be consistent with the presence of weak inter-cluster antiferromagnetic interactions.

Despite the high values of the spin ground state of the Fe_{19} clusters the height of the barrier remains smaller than that observed in other single molecule magnets due to the very weak magnetic anisotropy. We are currently studying other derivatives with longer aliphatic chains on the heidi ligands in order to increase the distance and therefore decrease the interaction between clusters. This would allow a more accurate estimation of the magnetic anisotropy. Then the next challenge is to modify the properties of the cores of these systems in order to enhance their magnetic properties.

Conclusion

We have shown how it is possible to engineer both the crystal packing and magnetic properties of Fe_{19} oxyhydroxide clusters, through small variations on the encapsulating ligands. In this case, changing an H atom on the alcohol side chain of the parent ligand, to a Me or an Et group, results in a dramatic change in the hydrogen bonding of the lattice, leading to the formation of parallel stacks of Fe_{19} clusters. We also observe that the apparent overall ground state spin on the clusters decreases slightly in the order H > Me > Et, and suggest that this may be a consequence of subtle changes in the zero-field splitting and inter-cluster antiferromagnetic interactions. It is also likely that as the chain length increases there will be a tendency for the disks to order into more regular hexagonal arrays. We are currently studying longer chain derivatives to

investigate these suggestions. All these systems can be regarded as single molecule magnets and we have shown how it is possible to vary supramolecular interactions in order to produce nanostructured arrays of magnetic particles.

Acknowledgements

We thank the Royal Society for the provision of a University Research fellowship to one of us (S. L. H.) and the EPSRC for the provision of a studentship (J. C. G.). The financial support of Ministero dell'Università e della Ricerca Scientifica e Tecnologica and of the European TMR program (contract no. ERBFMGECT950077) is gratefully acknowledged.

References

1 O. Kahn, *Science*, 1998, **279**, 44.
2 D. Gatteschi, A. Caneschi, L. Pardi and R. Sessoli, *Science*, 1994, **265**, 1054; F. E. Mabbs, E. J. L. McInnes, M. Murrie, S. Parsons, G. M. Smith, C. C. Wilson and R. E. Winpenny, *Chem. Commun.*, 1998, 643; K. Dimitrou, A. D. Brown, K. Folting and G. Christou, *Inorg. Chem.*, 1999, **38**, 1834; S. M. J. Aubin, N. R. Dilley, L. Pardi, J. Krzystek, M. W. Wemple, L.-C. Brunel, M. B. Maple, G. Christou and D. N. Hendrickson, *J. Am. Chem. Soc.*, 1998, **120**, 4991.
3 S. L. Heath and A. K. Powell, *Angew. Chem.*, *Int. Ed. Engl.*, 1992, **31**, 191.
4 A. K. Powell, S. L. Heath, D. Gatteschi, L. Pardi, R. Sessoli, G. Spina, F. Del Giallo and F. Pieralli, *J. Am. Chem. Soc.*, 1995, **117**, 2491.
5 D. J. Price, F. Lionti, R. Ballou, P. T. Wood and A. K. Powell, *Philos. Trans. R. Soc. London*, *Ser. A*, 1999, **357**, 3099.
6 W. Wernsdorfer, E. B. Orozco, K. Hasselbach, A. Benoit, B. Barbara, N. Demoncy, A. Loiseau, H. Pascard and D. Mailly, *Phys. Rev. Lett.*, 1997, **78**, 1791.
7 A. L. Barra, P. Debrunner, D. Gatteschi, Ch. E. Schulz and R. Sessoli, *Europhys. Lett.*, 1996, **35**, 133; R. Sessoli, D. Gatteschi, A. Caneschi and M. A. Novak, *Nature* (*London*), 1993, **365**, 141; F. Muller, M. A. Hopkins, N. Coron, M. Grynberg, L. C. Brunel and G. Martinez, *Rev. Sci. Instrum.*, 1989, **60**, 3681.
8 G. M. Sheldrick, SHELXL-97, an integrated system for solving and refining crystal structures from diffraction data, University of Göttingen, 1997.
9 A. L. Barra, L. C. Brunel, D. Gatteschi, L. Pardi and R. Sessoli, *Acc. Chem. Res.*, 1998, **31**, 460.
10 A. Caneschi, D. Gatteschi, C. Sangregorio, R. Sessoli, L. Sorace, A. Cornia, M. A. Novak, C. Paulsen and W. Wernsdorfer, *J. Magn. Magn. Mater.*, 1999, **200**, 182.